Gastric Cancer (2013) 16:355–361
DOI 10.1007/s10120-012-0194-x

ORIGINAL ARTICLE

Usefulness of three-dimensional angiographic analysis of perigastric vessels before laparoscopic gastrectomy

Ichirota Iino · Takanori Sakaguchi · Hirotoshi Kikuchi · Shinichiro Miyazaki · Takeshi Fujita · Yoshihiro Hiramatsu · Manabu Ohta · Kinji Kamiya · Takasuke Ushio · Yasuo Takehara · Hiroyuki Konno

Received: 9 April 2012 / Accepted: 14 August 2012 / Published online: 11 September 2012

Abstract
Background Recognition of perigastric vessel anatomy is important to safely perform gastric surgery, especially in the case of laparoscopic gastrectomy. This study was designed to reevaluate the efficacy of preoperative three-dimensional (3D) angiography reconstructed from enhanced multidetector-row computed tomography (MDCT) data and to classify right gastric artery (RGA) branching patterns.
Methods Perigastric vessel anatomy was preoperatively analyzed using MDCT-based 3D angiography reconstructed by computer software in patients undergoing laparotomic ($n = 75$) and laparoscopic ($n = 25$) gastrectomy. Results were compared with intraoperative findings in all cases, and were also compared with maximum intensity projection (MIP) imaging, which is similar to conventional angiography, in 10 patients.
Results Preoperative diagnoses by 3D angiography were identical to intraoperative findings. The rates of branching patterns of the celiac artery and left gastric vein were comparable with previous reports. The detection rate of the right gastric artery (RGA) was 77.0 %. Branching patterns of the hepatic artery were classified into four types: right hepatic artery (RHA) + left hepatic artery (LHA) type, replaced RHA + LHA type, RHA + replaced LHA type, and replaced RHA + replaced LHA type. RGA ramification patterns were classified into three types according to hepatic arterial running patterns: distal (68.8 %), proximal (14.3 %), and caudal (16.9 %). Because of vessel overlapping, RGA ramified points were misdiagnosed under MIP images in two of ten cases (20 %).
Conclusions Preoperative 3D angiography is useful for a new system of classifying RGA ramification patterns into three types. With this system, surgeons can perform laparoscopic gastrectomy with lymph node dissection more safely.

Keywords Gastrectomy · Surgical anatomy · 3D angiography

I. Iino (✉) · T. Sakaguchi · H. Kikuchi · S. Miyazaki · T. Fujita · Y. Hiramatsu · M. Ohta · K. Kamiya · H. Konno
Second Department of Surgery, Hamamatsu University School of Medicine, 1-20-1 Handayama, Higashi-ku, Hamamatsu 431-3192, Japan
e-mail: iiino@hama-med.ac.jp

T. Ushio · Y. Takehara
Department of Radiology, Hamamatsu University School of Medicine, 1-20-1 Handayama, Higashi-ku, Hamamatsu 431-3192, Japan

Introduction

Laparoscopic surgery for gastric malignancies has been gradually accepted in recent years because of its advantages over open surgery, including minimal invasiveness, less bleeding, less pain, and better cosmetic results [1–3]. To safely perform laparoscopic surgery, good skills and experience are absolutely essential.

Lymph node metastasis occurs in approximately 20 % of submucosal gastric cancers [4, 5]. Therefore, lymphadenectomy is necessary, even for early-stage gastric cancer [6, 7]. To completely dissect lymph nodes, the artery around the stomach should be exposed by manipulation. Laparoscopic lymph node dissection is difficult because of the two-dimensional view and a lack of tactile sensation [8]. For these reasons, it would be beneficial to determine perigastric vessel anatomy preoperatively for the safe performance of laparoscopic gastrectomy.

Recent advances in three-dimensional (3D) computed tomography have enabled the examination of vascular anatomy without percutaneous catheter angiography. Some authors have reported the usefulness of 3D angiography for the detection of perigastric vessels, such as the left gastric artery (LGA) and left gastric vein (LGV), before laparoscopic gastrectomy [9–12]. Furthermore, Kawasaki et al. showed that the LGV was identified in 93.8 % of cases, even by multidetector computed tomography alone without 3D angiography [13]. Although thick arteries, such as the branches of the celiac artery, including the LGA, are easily visualized with or without 3D angiography, it is difficult to detect thinner vessels with more complicated ramification, such as the right gastric artery (RGA) [11].

In this study, we reevaluated the efficacy of preoperative 3D angiography of perigastric vessels, especially for detection of the RGA, and report a novel classification of RGA branching patterns.

Materials and methods

Patients

This study included 100 consecutive patients undergoing multidetector-row computed tomography (MDCT) between April 2009 and October 2010 before gastric surgery. The patient population consisted of 71 men and 29 women from 26 to 86 years of age (median age, 67 years). Ninety-eight patients had gastric cancer and 2 had gastric gastrointestinal stromal tumors.

Computed tomography protocol

The protocol used in this study is described in our previous report [14]. Images were obtained using an Aquillion MULTI 64-MDCT scanner (Toshiba Medical Systems, Tokyo, Japan). A 20-G intravenous catheter was inserted from the medial cubital vein. A range of contrast-enhanced computed tomography (CT) scans was set to cover the area from the dome of the liver to the aortic bifurcation. With contrast-enhanced CT images, a nonionic contrast agent (370 mg or 300 mg I/ml, Omnipaque; Daiichi Pharmaceutical, Tokyo, Japan) was infused rapidly at a rate of 40 mg I/kg for 25 s using an automated injector. Early arterial phase images were obtained using the bolus tracking method. In brief, early arterial phase scanning started when Hounsfield units reached 200 in the abdominal aorta at the level of bifurcation of the celiac artery. The average scanning delay between the start of contrast material injection and the start of early arterial phase scanning was 20 s (range 15–28 s). Late arterial phase scanning and early venous phase scanning were started 10 and 30 s, respectively, after early arterial phase scanning.

Three-dimensional angiography by workstation

Volume data were transferred to a workstation (ZIOSTATION; Zio Software, Tokyo, Japan). Arteriography was obtained from early arterial phase scanning data. Portography was prepared either from the late arterial phase or from the early venous phase. Arteriography and portography were subsequently fused.

Results

Branching patterns of the celiac artery and running aspects of the LGV

To reevaluate the efficacy of 3D angiography, the celiac artery and LGV were visualized. Branching patterns of the celiac artery were classified according to Adachi's classification [15]: type I, common trunk of the LGA, the splenic artery (SPA), and the common hepatic artery (CHA); type II, common trunk of the SPA and CHA; type III, common trunk of the CHA, SPA, and the superior mesenteric artery (SMA); type IV, common trunk of the LGA, SPA, CHA, and SMA; type V, common trunk of the LGA and SPA, and another common trunk of the CHA and SMA; and type VI, common trunk of the LGA and SPA, and without representative CHA. Figure 1 shows representative 3D images of the branching pattern. Eighty-five patients were classified into type I (Fig. 1a), 8 into type II (Fig. 1b), 1 into type V (Fig. 1c), and 4 into type VI (Fig. 1d). In 2 of 8 patients classified into type II, the replaced left hepatic artery (LHA) branched from the aorta-derived LGA. Apart from 98 classifiable patients, 2 cases (Fig. 1e, f) were miscellaneous. In 1 patient, the LGA, SPA, and the LHA separately branched from the aorta, and the replaced right hepatic artery (RHA) was derived from the SMA (Fig. 1e). In another patient, the LGA was lost, but the RGA nourished the lesser gastric curvature (Fig. 1f), and the missing LGA was confirmed intraoperatively.

The LGV was visualized in 89 (89.0 %) of 100 patients. We classified LGV joining patterns according to our previous classification [14]. The LGV joined the portal vein (type P) in 46 (51.7 %) cases, the splenic vein (type SP) in 30 (33.7 %) cases, and the splenoportal confluence (type C) in 13 (14.6 %) cases. In type P, the LGV preferentially ran along the dorsal side of the CHA in 40 (87.0 %) cases. In type SP, the LGV preferentially ran along the ventral side of the SPA ($n = 12$), the celiac axis ($n = 6$), or the CHA ($n = 4$) in 22 (73.3 %) cases. In type C, the LGV preferentially ran along the ventral side of the CHA ($n = 7$), SPA

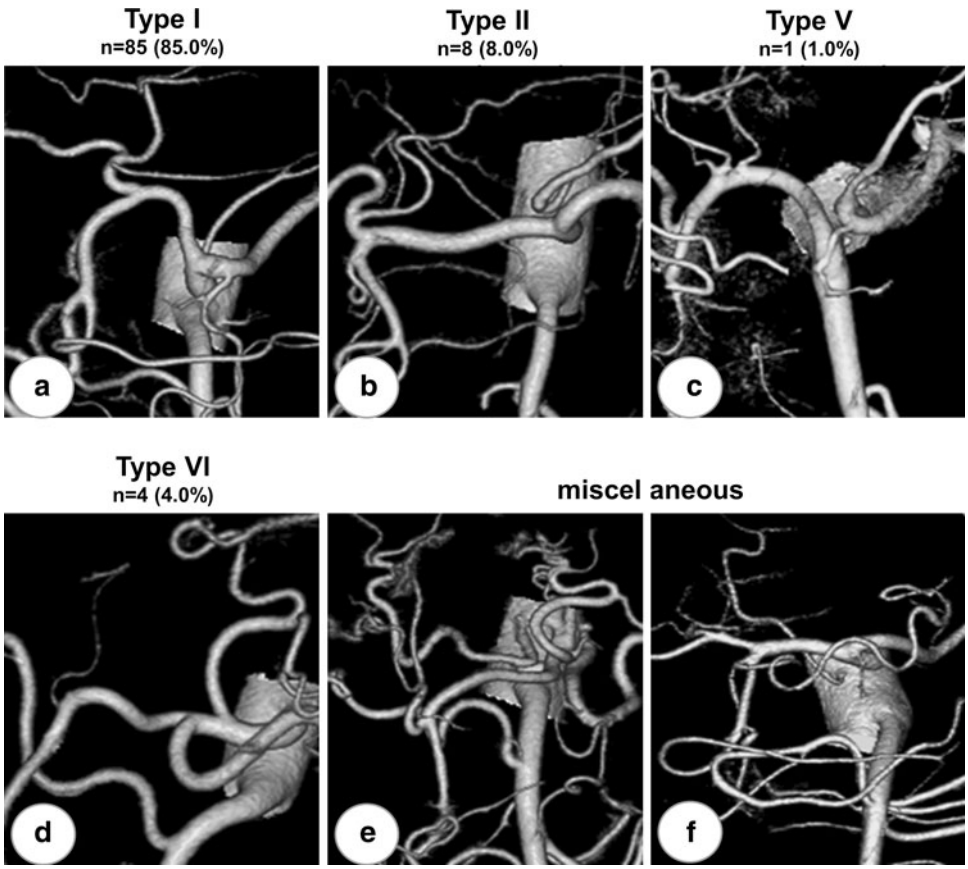

Fig. 1 Representative three-dimensional (3D) images of the branching pattern of the celiac artery according to Adachi's classification. **a** Type I (normal branch): common trunk of the left gastric artery (LGA), splenic artery (SPA), and common hepatic artery (CHA). **b** Type II: common trunk of the SPA and CHA. The LGA is directly derived from the aorta. **c** Type V: common trunk of the LGA and SPA, and another common trunk of the CHA and superior mesenteric artery (SMA). **d** Type VI: common trunk of the LGA and SPA, and without representative CHA. **e**, **f** Two cases were miscellaneous. In **e**, the LGA, SPA, and left hepatic artery (LHA) were separately branched from the aorta and the replaced right hepatic artery (RHA) was derived from the SMA. In **f**, LGA was unidentified, but the right gastric artery (RGA) nourished the lesser gastric curvature. In this case, the missing LGA was confirmed intraoperatively

Table 1 Branching types of the right gastric artery (RGA) on 3D angiography in 100 patients

Hepatic artery ramification	Total	RGA ramified from						RGA unidentified
		Distal			Proximal		Caudal	
		RHA	LHA	PHA	BP	CHA	GDA	
RHA + LHA	82	2	13	30	5	1	12	19
Replaced RHA + LHA	10	0	6	–	1	0	0	3
RHA + replaced LHA	5	2	0	–	3	0	0	0
Replaced RHA + replaced LHA	3	0	0	–	1	0	1	1
Total	100	4	19	30	10	1	13	23
		53 (68.8 %)			11 (14.3 %)		13 (16.9 %)	

RGA right gastric artery, *RHA* right hepatic artery, *LHA* left hepatic artery, *PHA* proper hepatic artery, *BP* branching point of gastroduodenal artery, *CHA* common hepatic artery, *GDA* gastroduodenal artery

($n = 2$), or CHA–SPA bifurcation point ($n = 2$) in 11 (84.6 %) cases.

A novel classification of branching patterns of the RGA

As shown in Table 1, the RGA was identified in 77 cases (77.0 %). As earlier studies had neglected hepatic arterial anomalies in the analysis of RGA ramification points [11, 16], we precisely examined RGA ramification according to hepatic arterial running patterns. First, branching patterns of the hepatic artery were classified into four types: RHA + LHA type, both being derived from the proper hepatic artery (PHA) (Fig. 2a, $n = 82$); the replaced RHA + LHA type, with the replaced RHA coming from the SMA or celiac artery and the LHA from the CHA (Fig. 2b, $n = 10$); the RHA + replaced LHA type, where the RHA comes from the CHA and the replaced LHA from the LGA (Fig. 2c, $n = 5$); the replaced RHA + replaced

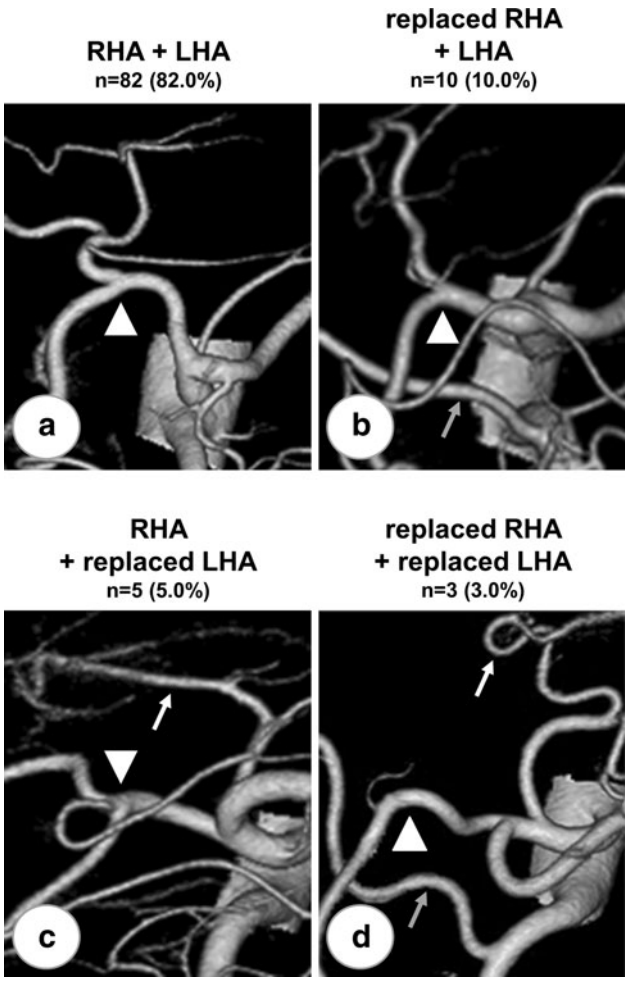

Fig. 2 Various patterns of hepatic arteries on 3D angiography. The branching point of the GDA is named the "branching point (BP)" (*arrowhead*). **a** RHA + LHA type: both the RHA and LHA are from the proper hepatic artery (PHA). **b** Replaced RHA + LHA type: the replaced RHA is from the SMA (*gray arrow*) and the LHA is from the CHA. **c** RHA + replaced LHA type: the RHA is from the CHA, and the replaced LHA is from the LGA (*white arrow*). **d** Replaced RHA + replaced LHA type: the replaced RHA is from the SMA (*gray arrow*), and the replaced LHA is from the LGA (*white arrow*). In the last case, the GDA directly branches from the so-called CHA

LHA type, where the replaced RHA comes from the SMA and the replaced LHA from the LGA (Fig. 2d, $n = 3$). In the replaced RHA + replaced LHA type, the gastroduodenal artery (GDA) directly branches from the so-called CHA. The root of the GDA was defined as the "branching point (BP)." The RGA ramification patterns were then classified into three types: the distal type, in which the RGA ramifies from the distal arteries (PHA, RHA, and LHA) relative to the BP; the proximal type, in which the RGA ramifies from the CHA or BP; and the caudal type, in which the RGA ramifies from the GDA (Figs. 2, 3). In the replaced RHA + replaced LHA type, the rightward turning point (so-called CHA) to the point of descent (so-called GDA) was defined as the BP (Fig. 2d). According to these definitions, 53 RGAs (68.8 %) were classified into the distal type (Fig. 3a), 11 (14.3 %) into the proximal type (Fig. 3b), and 13 (16.9 %) into the caudal type (Fig. 3c). The relationships between hepatic artery ramification type and RGA ramification type are shown in Table 1.

Comparison between 3D angiography and MIP imaging

The superiority of 3D angiography to conventional angiography is its ability to avoid vessel overlapping [16]. Therefore, 3D angiography was compared with MIP images, which were very similar to angiographic anterior (ventrodorsal) views. Figure 4a represents typical MIP images, in which the RGA appears to be from the CHA. Figure 4b shows 3D angiography obtained from the same patient, and it clearly visualized the RGA BP (from the PHA). In another patient, the RGA BP was obscure in MIP images (Fig. 4c), as well as in 3D angiographic anterior views (Fig. 4d). The right anterior 3D angiographic view clearly visualized the PHA-derived RGA (Fig. 4e). In total, RGA BPs were misdiagnosed under MIP images in two of ten patients (20 %). These findings suggest that 3D angiography is superior to conventional angiography and may be necessary for the accurate diagnosis of RGA BPs.

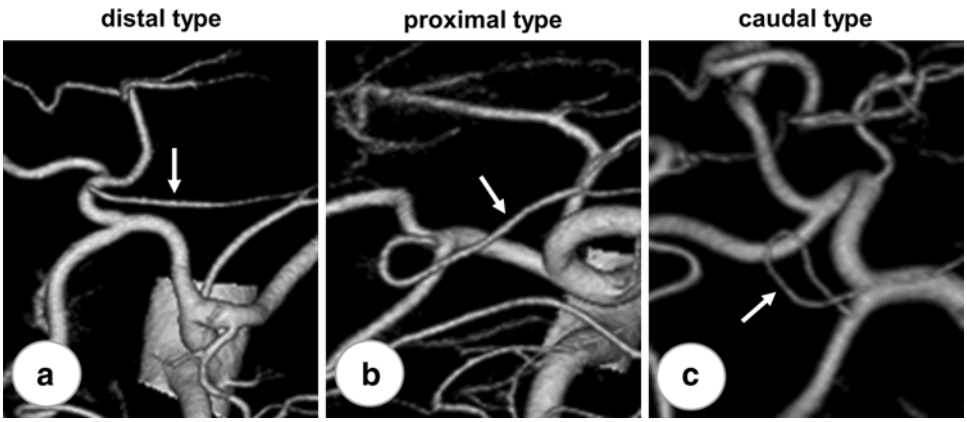

Fig. 3 Right gastric artery (RGA) ramification patterns. **a** Distal type ($n = 45$) in which the RGA ramifies from distal arteries relative to the BP. **b** Proximal type ($n = 6$) in which the RGA ramifies from the CHA or the BP. **c** Caudal type ($n = 12$) in which the RGA ramifies from the gastroduodenal artery (GDA). *Arrows* indicate the RGA

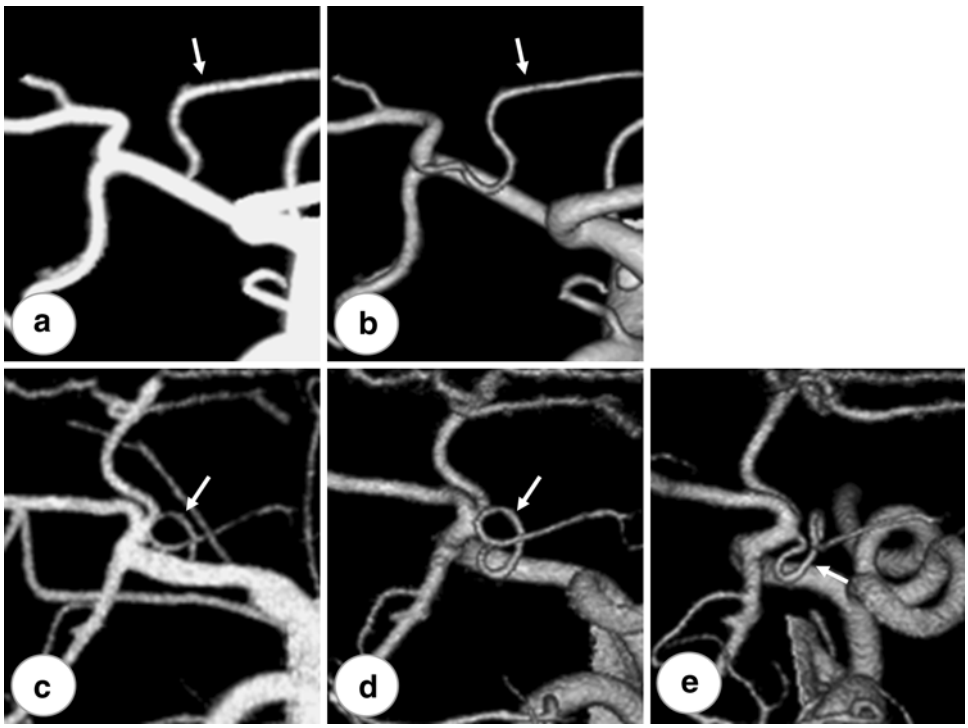

Fig. 4 Comparison of maximum intensity projection (MIP) images with 3D angiography. **a** In MIP images, the RGA appears to be from the CHA. **b** Three-dimensional (3D) angiography obtained from the same patient in **a**. RGA branching from the PHA can be clearly visualized. **c** In another case, the RGA branching point was obscure in MIP images. **d** The branching point was also unclear in 3D angiographic views from the same direction as **c**. **e** The RGA branching point (from PHA) is clearly shown by a different directional view. *Arrows* indicate the RGA

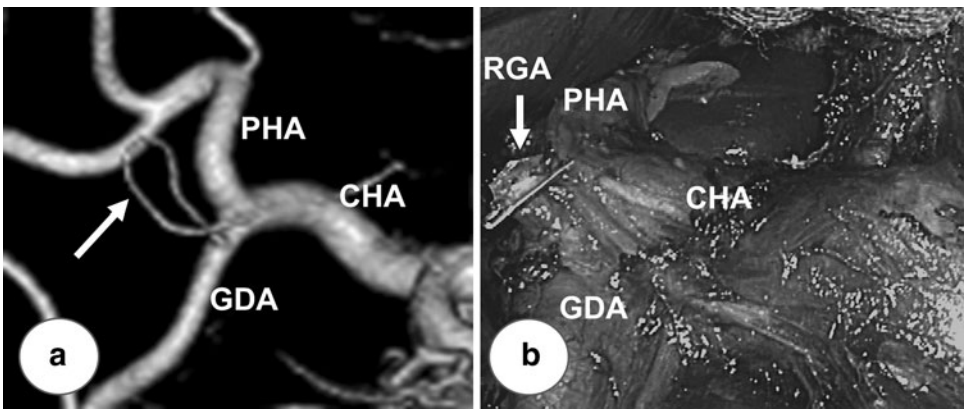

Fig. 5 Comparison of 3D angiographic images and laparoscopic views. **a** This patient had a caudally branched RGA. **b** Intraoperatively, the stump of the RGA was below the CHA–PHA–GDA branching point

Comparison between preoperative 3D angiographic results and intraoperative findings

The running aspects of perigastric vessels were intraoperatively observed. Preoperative 3D angiographic results were identical to intraoperative findings. A typical case of a patient with gastric cancer is shown in Fig. 5. In this case, we preoperatively determined a caudally ramified RGA under 3D angiography (Fig. 5a). This arterial branch was skeletonized under laparoscopic surgery (Fig. 5b).

Discussion

In this study, we analyzed perigastric vessel anatomy using 3D angiography reconstructed from enhanced MDCT data. Importantly, 3D angiographic results were identical to intraoperative findings. The rate of branching patterns of the celiac artery was 86.7 % in Adachi's type I, 8.2 % in type II, 1.0 % in type V, and 4.1 % in type VI. In the analysis of the LGV, the rates of types P, SP, and C were 51.7, 33.7, and 14.6 %, respectively. These data are comparable with a previous report, suggesting that 3D angiography in the present study was reliable, and the data reconfirmed the rate of major vessel branching patterns.

The importance of preoperative information of vessel anatomy has been accepted since the era of interventional percutaneous angiography. Thick arteries, such as the LGA, are easily analyzed, but thinner and complicated branched arteries, such as the RGA, are hard to identify, even under conventional percutaneous angiography. The detection rate of the RGA in angiography was reported to

be 44 % [17], presumably because of its inability to avoid vessel overlapping. In contrast to conventional angiography, MDCT-based 3D angiography enables angle-free observations to be performed. The RGA detection rate of this method was approximately 53.7–100 % in previous reports [8–11] and 77 % in the current study, suggesting the superiority of MDCT-based 3D angiography to conventional angiography. However, in the present study, the RGA detection rate was only 40.9 % (9/22) during the initial 4 months. Its rate increased to 72.7 % (16/22) during the next 4 months, and finally reached 91.9 % (51/56) during the subsequent 10 months. This increase implies that training and increased knowledge of perigastric vessel anatomy makes it easier to analyze thinner and complicated vessels.

In the present study, we classified the RGA ramification pattern into three types: distal, caudal, and proximal (Table 1). We first examined hepatic arterial running patterns to better understand RGA ramification points by determining the relationship to BPs. The frequencies of each RGA ramification point in the present study are different from those found in other studies. In our study, 53 RGAs (68.8 %) were ramified distally, 11 (14.3 %) proximally, and 13 (16.9 %) caudally. In contrast, RGAs were ramified at distal, caudal, and proximal arteries, accounting for 75.0, 25.0, and 0 %, respectively, in conventional angiographic analysis reported by Lunderquist [17]. An important point to note based on the current study findings is that RGA ramification points are sometimes misdiagnosed under MIP imaging, which is very similar to angiographic anterior views. Such misdiagnosis and, perhaps, at least in part, race differences could account for the differences between their results and our study.

When the RGA is dissected during laparoscopic gastrectomy, it is important to manipulate the RGA differently according to the RGA ramification points. The RGA can be dissected either before or after dissection of the bulbus in the case of laparotomic gastrectomy, because the RGA is easily identified by free mobilization of the antrum and bulbus, irrespective of RGA ramification points. In contrast, in the case of laparoscopic gastrectomy, because mobilization of the stomach is restricted, it is sometimes difficult to detect a caudally or proximally ramified RGA. Kanaya et al. [18] defined a layer between fat tissue, including lymph nodes and nerve fascicle around the main artery, such as the common hepatic artery or splenic artery, as the "outmost layer," and reported that keeping the outmost (outermost) layer of the nerves is important when dissecting suprapancreatic lymph nodes. The outmost layer has been reported to be easily found at the root of the LGA, but it is relatively difficult to approach the layer at the lateral side [18]. When dissecting suprapancreatic lymph nodes on the right side, a caudally or proximally ramified RGA may make it difficult to accurately find the outmost layer and may cause unexpected blood loss during dissection. Therefore, preoperative 3D angiography could help surgeons more safely perform laparoscopic gastrectomy with lymph node dissection by accurately picturing vessel anatomy, including RGA ramification patterns.

In conclusion, 3D analysis of perigastric vessels, with its angle-free spatial observation, can accurately classify RGA ramification patterns into three new types: distal, proximal, and caudal. Preoperative 3D information about the perigastric vessels, including RGA ramification patterns, may help surgeons safely perform laparoscopic gastrectomy with lymph node dissection.

References

1. Adachi Y, Shiraishi N, Shiromizu A, Bandoh T, Aramaki M, Kitano S. Laparoscopy-assisted Billroth I gastrectomy compared with conventional open gastrectomy. Arch Surg. 2000;135:806–10.
2. Shimizu S, Uchiyama A, Mizumoto K, Morisaki T, Nakamura K, Shimura H, et al. Laparoscopically assisted distal gastrectomy for early gastric cancer: is it superior to open surgery? Surg Endosc. 2000;14:27–31.
3. Kitano S, Shiraishi N, Fujii K, Yasuda K, Inomata M, Adachi Y. A randomized controlled trial comparing open vs. laparoscopy-assisted distal gastrectomy for the treatment of early gastric cancer: an interim report. Surgery (St. Louis). 2002;131:S306–11.
4. Nakamura K, Morisaki T, Sugitani A, Ogawa T, Uchiyama A, Kinukawa N, et al. An early gastric carcinoma treatment strategy based on analysis of lymph node metastasis. Cancer (Phila). 1999;85(7):1500–5.
5. Kurihara N, Kubota T, Otani Y, Ohgami M, Kumai K, Sugiura H, et al. Lymph node metastasis of early gastric cancer with submucosal invasion. Br J Surg. 1998;85:835–9.
6. Bonenkamp JJ, Hermans J, Sasako M, van de Velde CJ. Extended lymph-node dissection for gastric cancer. N Engl J Med. 1999;340(12):908–14.
7. Yang SH, Zhang YC, Yang KH, Li YP, He XD, Tian JH, et al. An evidence-based medicine review of lymphadenectomy extent for gastric cancer. Am J Surg. 2009;197(2):246–51.
8. Kumano S, Tsuda T, Tanaka H, Hirata M, Kim T, Murakami T, et al. Preoperative evaluation of perigastric vascular anatomy by 3-dimensional computed tomographic angiography using 16-channel multidetector-row computed tomography for laparoscopic gastrectomy in patients with early gastric cancer. J Comput Assist Tomogr. 2007;31(1):93–7.
9. Matsuki M, Kani H, Tatsugami F, Yoshikawa S, Narabayashi I, Lee SW, et al. Preoperative assessment of vascular anatomy around the stomach by 3D imaging using MDCT before laparoscopy-assisted gastrectomy. Am J Roentgenol. 2004;183(1):145–51.
10. Matsuki M, Tanikake M, Kani H, Tatsugami F, Kanazawa S, Kanamoto T, et al. Dual-phase 3D CT angiography during a single breath-hold using 16-MDCT: assessment of vascular anatomy before laparoscopic gastrectomy. Am J Roentgenol. 2006;186(4):1079–85.
11. Fujiwara M, Kodera Y, Satake H, Misawa K, Miura S, Nakayama G, et al. Navigation for laparoscopic gastrectomy with 3-dimensional computed tomography (3D-CT). Hepatogastroenterology. 2008;55(85):1201–5.

12. Natsume T, Shuto K, Yanagawa N, Akai T, Kawahira H, Hayashi H, et al. The classification of anatomic variations in the perigastric vessels by dual-phase CT to reduce intraoperative bleeding during laparoscopic gastrectomy. Surg Endosc. 2011;25:1420–4.
13. Kawasaki K, Kanaji S, Kobayashi I, Fujita T, Kominami H, Ueno K, et al. Multidetector computed tomography for preoperative identification of left gastric vein location in patients with gastric cancer. Gastric Cancer. 2010;13:25–9.
14. Sakaguchi T, Suzuki S, Morita Y, Oishi K, Suzuki A, Fukumoto K, et al. Analysis of anatomic variants of mesenteric veins by 3-dimensional portography using multidetector-row computed tomography. Am J Surg. 2010;200(1):15–22.
15. Adachi B. Das Arteriensystem der Japaner, vol. 2. Tokyo: Maruzen; 1928.
16. Lee SW, Shinohara H, Matsuki M, Okuda J, Nomura E, Mabuchi H, et al. Preoperative simulation of vascular anatomy by three-dimensional computed tomography imaging in laparoscopic gastric cancer surgery. J Am Coll Surg. 2003;197(6):927–36.
17. Lunderquist A (1967) Arterial segmental supply of the liver. An angiographic study. Acta Radiol Diagn (Stockh) (Suppl) 272:1–81
18. Kanaya S, Haruta S, Kawamura Y, Yoshimura F, Inaba K, Hiramatsu Y, et al. Laparoscopy distinctive technique for suprapancreatic lymph node dissection: medial approach for laparoscopic gastric cancer surgery. Surg Endosc. 2011;25:3928–9.